STUDY OF FLEXURAL BEHAVIOUR OF ECC FERROCEMENT I-BEAM

PROJECT REPORT

Submitted by

AJMAL S N

TKM21CESC01

To

the A P J Abdul Kalam Technological University

in partial fulfilment of the requirements for the award of the Degree

of

Master of Technology

In

Structural Engineering & Construction Management

DEPARTMENT OF CIVIL ENGINEERING

T.K.M. College of Engineering, Kollam

July 2023

DEPARTMENT OF CIVIL ENGINEERING

T K M COLLEGE OF ENGINEERING, KOLLAM

CERTIFICATE

Certified that this report entitled **'STUDY OF FLEXURAL BEHAVIOUR OF ECC FERROCEMENT I-BEAM'** is the report of the project presented by **AJMAL S N, TKM21CESC01** during **2022-2023** in partial fulfilment of the requirements for the award of the Degree of Master of Technology in Structural Engineering & Construction Management of the A P J Abdul Kalam Technological University.

Guide	Project Coordinator	Head of the Department
Prof. Mohammed Thowsif	**Dr. Kavitha Madhu**	**Dr. Sajeeb R**
Assistant Professor	Associate Professor	Professor
Dept. of Civil Engg.	Dept. of Civil Engg.	Dept. of Civil Engg.

ACKNOWLEDGEMENT

I take this opportunity to express my deep sense of gratitude and sincere thanks to all who helped me to do the project successfully.

I am deeply indebted to my guide, **Mr. Mohammed Thowsif,** Assistant Professor, Department of Civil Engineering, for his excellent guidance, positive criticism and valuable comments.

I am greatly thankful to my project coordinators, **Dr. Kavitha Madhu**, Associate Professor, Department of Civil Engineering, for her constant supervision as well as for providing necessary information regarding the project.

I am greatly thankful to **Dr. Sajeeb R**, Professor and Head of the Department of Civil Engineering, for his kind support.

Finally, I thank my parents and friends who directly and indirectly contributed to the successful completion of my project.

AJMAL S N

ABSTRACT

Due to its poor crack width control, limited flexural behaviour, delamination of mortar, etc., the use of ferrocement as a structural element is restricted. Utilizing ferrocement in construction will assist reduce the overall weight of the building, hence lowering its inertia. The key benefit is that using ferrocement can lower the overall cost of building, as material costs, labour costs, and storage costs make up the majority of the entire cost. In this study, I-beams made of ferrocement are cast, their flexural properties are evaluated, and it is determined whether they are a good alternative to traditional beams for use in residential building construction. Ferrocement I-beams made of standard mortar mix have been cast and tested; a second group of I-beams casted using Engineering Cementitious Composites (ECC) instead of standard mortar mix, and the difference in behaviour will be examined. ECC ferrocement I-beam showed better load carrying capacity, crack resistance, energy absorption and ductility index.

TABLE OF CONTENTS

LIST OF FIGURES

LIST OF TABLES

LIST OF ABBREVIATIONS

SC ECC	Self-Compacting Engineering Cementitious Composites
HRWR	High Range Water Reducer

Chapter 1

Introduction

1.1 General

The recent rapid increase in building costs, both in residential and commercial construction, can primarily be attributed to the rising prices of materials and labor. Additionally, an often overlooked factor that significantly affects overall building costs is the expense associated with material storage. To mitigate these increasing costs, the industry is exploring the use of cost-effective materials and adopting economical construction techniques.

In this context, ferrocement construction has emerged as a promising solution for reducing the expenses associated with residential building construction. Ferrocement is known for its versatility in producing complex shapes that are challenging to achieve with other materials. Moreover, it is commonly used to strengthen or rehabilitate structural members such as walls, columns, and beams by applying a layer of ferrocement, known as jacketing. Furthermore, ferrocement finds applications in significant fields such as silos and water pipe construction.

However, despite its cost-effectiveness, ferrocement is not commonly employed as a primary structural element in buildings due to certain limitations. For instance, its flexural behavior is limited, which restricts its application as a load-bearing beam in a structure. Moreover, ferrocement exhibits poor control over crack width, which can result in increased water permeability and exposure of the reinforcing mesh to moisture and corrosive agents. This, in turn, can lead to corrosion and significantly reduce the service life of the structural member and the entire structure.

To overcome these limitations, it is crucial for a material to demonstrate favorable flexural behavior when utilized as a structural component. Additionally, effective crack width control is essential to minimize water permeability and the risk of corrosion. While ferrocement offers cost advantages, careful consideration must be given to its limitations, ensuring appropriate use within the overall structural system to maximize its benefits and minimize potential drawbacks.

By understanding the advantages and limitations of ferrocement, the construction industry can make informed decisions regarding its application in residential building construction, striking a balance between cost-effectiveness and structural performance.

1.2 Engineering cementitious composites

Engineering Cementitious Composites (ECC) is an Ultra High Performance Fibre Reinforced Cementitious Composite (UHPFCC) that offers superior ductility compared to traditional concrete or mortar. ECC is often referred to as "bendable concrete" due to its exceptional multiple cracking behavior and strain hardening effect. One of the key characteristics of ECC is its ability to develop microcracks, which play a significant role in reducing the permeability of the matrix. This reduction in permeability enhances the protection of the reinforcement within the composite, thereby extending the overall lifespan of the structural element.

The constituents of ECC typically include cement, fine silica sand, water, fibers, fly ash, and superplasticizer, with relatively high proportions of each component. Notably, coarse aggregate is omitted from the mixture to mitigate any negative effects on the ductility of the composite. Fly ash, a supplementary cementitious material can be partially substituted in ECC to enhance its ductility. This substitution weakens the bond between the matrix and the fibers, allowing for improved ductile behavior of the composite.

By carefully selecting and proportioning the constituents, ECC achieves a unique combination of enhanced ductility, multiple cracking behavior, and improved durability. This makes it a promising material for various applications where flexibility, crack control, and extended service life are critical factors. The exclusion of coarse aggregate and the inclusion of fly ash as a partial replacement contribute to the distinctive properties of ECC, enabling its successful application in a range of structural and construction projects.

Chapter 2

Literature review

2.1 Behaviour of Ferrocement

Abdullah et al (2022) studied the flexural behaviour of hollow self-compacted mortar ferrocement beam reinforced with various types of metallic bars like steel bars and steel wire mesh and non-metallic bars like Glass Fibre Reinforced Polymer (GFRP) bars and fiber glass mesh reinforcement. For the experimental purpose twenty ferrocement beams with dimensions 150 x 225 x 2000 mm and thickness 50mm. Properties of every materials including the mortar, steel bars, steel mesh, etc was evaluated. The load deflection relationship, ductility, ductility index of test beams, toughness, load-strain curves and crack pattern and failure mechanism of the beams were studied and understood. It was concluded that the usage of GFRP bars and several layers of fibre glass mesh used for reinforcement gave higher loads than thee beams reinforced with steel bars and several layers of steel wire mesh. And increase in number of wire meshes increase the first crack load, ultimate load and energy absorption capacity.

Dat et al (2022) investigated the impact of tension stiffening on the tensile and flexural behaviour of ferrocement with Engineering ECC. ECC mix consist of 2% Poly Vinyl Alcohol (PVA) fibre by volume and the super plasticizer used is polycarboxylate based. Welded wire mesh of diameter 1.2 mm and opening 12.5 mm was used. Specimens with varying number of layers of wire meshes were casted and tested. Tensile properties of the ferrocement specimens were examined using uniaxial tensile tests on the dog bone shaped specimens and the flexural behaviour also tested using four point bending test. The tensile behaviour including the failure pattern, stress-strain response and tension stiffening behaviour and the flexural behaviour were obtained. It was concluded that the ECC ferrocement had enhanced the strength and crack width control compared to conventional ferrocement, but the improvement in deformation capacity in limited. Also, the interaction between the steel mesh and the ECC developed a tension stiffening effect and improved the uniaxial and flexural strength.

Kaish et al (2012) investigated some improved ferrocement jacketing techniques for restrengthening of square reinforced concrete columns. Non jacketed columns (NJ), single layer wire mesh and sharp column corners (SL), single layer wire mesh and

rounded column corners (RSL), single layer wire mesh with shear keys at the centre of each face of column (SKSL) and single layer wire mesh and two extra layers mesh at each corner (SLTL) were cast with normal ties and seismic ties and tested under concentrated load and eccentric load. SLTL columns performed better in the case of ultimate load carrying capacity and RSL column showed better lateral deformation. All the jacketed columns performed better than non jacketed columns. Increase in number of layers of wire meshes improved the behaviour of columns.

2.2 High-Performance Mortar for Ferrocement

Dawood et al (2021) experimentally investigated the flexural performance of ferrocement based on sustainable high-performance mortar. The study aims to promote the practice of eco-friendly construction methods by researching on sustainable High Performance Mortar. Behaviour of mortar with the addition of different percentages of Natural Sisal Fibre (NSF) say in the range of 0.5 to 1.5 % was studied. Rheological characteristics like flowability and hardened properties like compressive strength, split tensile strength, flexural strength, flexural toughness, modulus of rupture, etc were obtained. Results shows that the use of 1% of NSF is beneficial for increasing the flexural strength, split tensile strength and elastic modulus evidently.

Sankar and Rajkumar (2019) carried out an experimental investigation on different high rich cement mortar for ferrocement application. The developed high rich mortar matrices contain diverse combos of silica fume and Metakaolin, and offer a great balance among flowability and rich. It was proven that growing high rich and achievable cement mortar incorporating various proportions of silica fume, Metakaolin, and superplasticizer via weight of cement appears to be viable. The combination containing a mixture of approximately 10% silica fume, 10% Metakaolin, and 3% superplasticizer at a water to cement ratio of 0.4 on weight foundation, exhibited 15% increase in compressive rich in comparison to control mixes without admixtures.

2.3 Ultra High Performance Concrete in Structural Engineering

Hung et al (2022) reviewed the developments and challenges for ultra-high-performance concrete (UHPC) in Structural Engineering. The review was focussed on material behaviour, bond between UHPC and steel reinforcing bars, steel reinforced UHPC (R/UHPC) tensile members, flexural behaviour and design of R/UHPC beams, shear

behaviour and design of R/UHPC beams, UHPC columns under axial compression, moment and shear, structural retrofitting and rehabilitation using UHPC and UHPC pavements. The author says that the UHPC flexural members exhibit enhanced cracking pattern, stiffness, and strength compared to equivalent RC members and the use of UHPC is effective in restraining the compression-associated failure patterns in regular RC members due to the ultrahigh compressive performance of UHPC in terms of strength, failure strain, confinement, and resistance to spalling and crushing.

Hung et al (2020) experimentally studied the workability and mechanical properties of UHPC with hooked end steel macro fibers. Fresh and hardened properties of the UHPC material was investigated. Mechanical properties of the hardened material was also studied. Results showed that addition of 1% by volume fraction of hooked end steel macro fibers increased the workability of the matrix and a reduction in workability was noted when the volume fraction of fibers changed to 2%. The inclusion of 1% volume fraction of hooked-end steel macro-fibers considerably reduced the compressive strength of UHPC by about 15% likely owing to the increased air content and micro-defects. When the volume fraction was further increased to 2%, the compressive strength was reversely increased slightly due to the enhanced confinement and crack control ability.

Hung et al (2021) studied the suitability of cast-in-place and prefabricated UHPC jackets for retrofitting shear-deficient reinforced concrete columns with different axial loads. Two control columns and five jacketed columns were used for the experimental programme. The jacketed columns include cast-in-place jackets with and without steel mesh and prefabricated jackets. The column specimens were tested using the Bi-Axial Testing System. The load displacement responses, reinforcement strain and failure modes were obtained. The results concluded that Steel reinforced UHPC jacketing increased the lateral strength of the shear-deficient columns by as high as 50%. And the inclusion of high-strength steel mesh in the UHPC jackets substantially improved the retrofitting performance because it enhanced the shear resistance, crack-controlled ability, and confinement of the UHPC jackets.

Sharma et al (2022) experimentally investigated initially damaged beam column joint retrofitted with reinforced ultra-high-performance hybrid fiber reinforced concrete (UHP-HFRC). Two control specimens and six beam column joint specimens were cast for the experimental program. The specimens were tested under quasi-static reversed cyclic

loading. Hysteresis behavior, ductility performance, stiffness and strength degradation, energy dissipation and crack pattern were analyzed in the program. The author concluded that The retrofitted specimens using reinforced UHP-HFRC overlay exhibited the improvement in the load-carrying capacity, ductility, drift capacity, energy dissipation, stiffness retention at higher drift, and lower strength degradation for a given damage level. The application of wire mesh to UHP-HFRC improves the overall performance and the author proposed to use welded wire mesh which is better than woven wire mesh.

Shao et al (2021) studied seismic performance of full-scale UHPC-jacket-strengthened reinforced concrete columns under high axial loads. The shear-deficient RC columns were constructed using the conventional concrete material provided by a ready-mixed concrete plant. The developed UHPC jacketing methods improved the lateral strength and drift capacity of the shear-deficient column by at least 40% and 30%, respectively. They also reduced the residual displacement of the column by 65%-80%.

2.4 Performance of ECC

Hung et al (2016) investigated on performance ECC jacketing in retrofitting shear-deficient reinforced concrete members. Six identical shear-deficient reinforced concrete structural members, cantilever beam specimens were prepared for the experimental program. Two of the specimens carry normal mortar and three of them carry ECC. One of the specimens is a control specimen. The specimens differ in number of layers of wire meshes. Results showed that all the retrofitting schemes of ECC jackets significantly improved the cyclic behavior of the original RC member, in terms of the strength, stiffness, ductility, energy dissipation capacity, shear distortion demand, and strain demand for the steel rebar and using ECC to replace the mortar in ferrocement reduced the crack width by an average of more than two times at all stages of loading and spalling has also removed.

Lepech and Li (2009) investigated on the water permeability of ECC. PVA fiber of 39-micrometer diameter and 12 mm length was used in the ECC. 26 kg/m^3 of PVA fiber was used in the matrix. Th specimens were subjected to permeability testing. The results showed that the design of an ECC composite which allowed for large tensile deformations while not sacrificing a low coefficient of permeability was completed. And when compared to reinforced mortar specimens cracked under uniaxial tension to 1.5% deformation, ECC material exhibits permeability up to six orders of magnitude lower.

Hu et al (2022) studied the local use of ECC to simultaneously enhance the shear strength and deformability of reinforced concrete beams. Compression-zone concrete was replaced with ECC in the experimental program. The shear strength contributions from concrete and stirrups were obtained. Results showed that the inclusion of ECC in the compression zone significantly increased both the shear strength and deformability of reinforced concrete beams. The ECC block in the compression zone exerted influences on the diagonal crack width, strain distribution of stirrups, shear modulus, and direction of the principal compressive strain.

2.5 Gaps Identified

From the literature, and surveys conducted the following gaps are identified.

- Extensive use of ferrocement as a structural member is limited
- Studies on ferrocement I-sections are limited
- Studies are limited in eliminating delamination in structural ferrocement elements

2.6 Objectives

- To determine the ultimate load carrying capacity of ferrocement I-beam for self compacting normal mortar mix and ECC mix
- To obtain the load deformation characteristics of the ferrocement I-beam
- To record and analyse the crack pattern developed on the beam section until failure

2.7 Scope

- Only I sections of ferrocement composite are cast and tested
- Durability of the composite is not tested
- Geometric parameters are kept constant
- Strength of mix shall be 40 N/mm^2

Chapter 3

Methodology

3.1 General

This chapter outlines the experimental plan and the materials utilised to create ferrocement I-beams from regular mortar mix and ECC in connection with the study. Material testing and tests for hardened specimens are part of the lab inquiry.

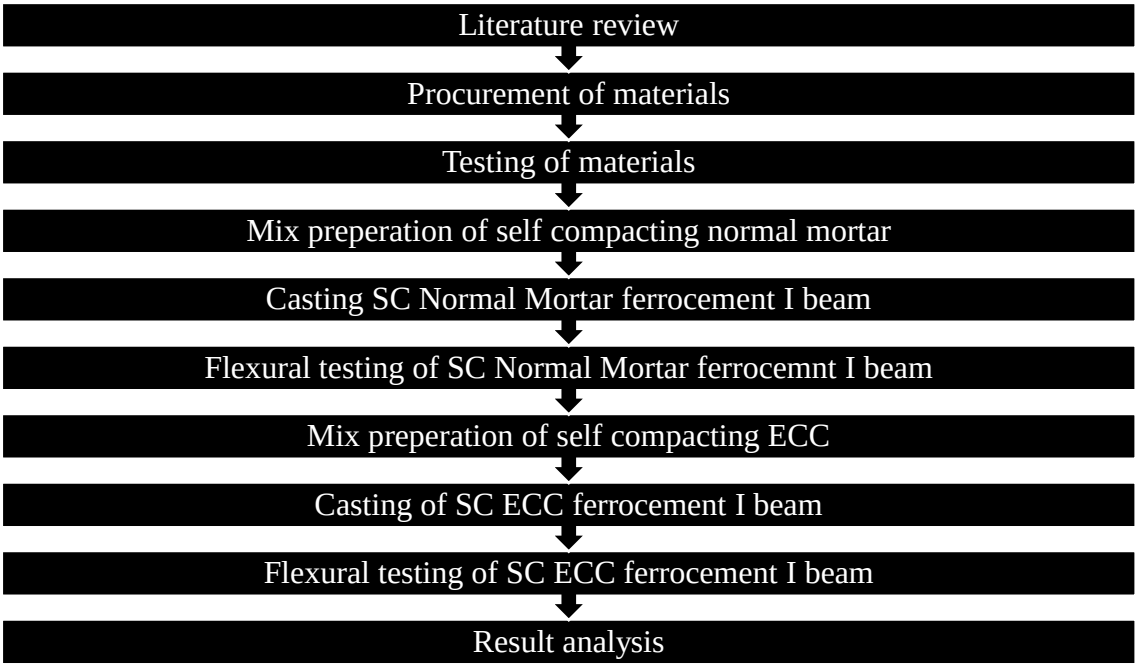

Figure 3.1 Methodology

3.2 Procurement of Materials

Different materials procured includes:

- Cement: 53 grade ordinary Portland cement (PPC) for casting specimens
- Manufactured sand as fine aggregates (FA)
- Class C Fly ash
- Potable water
- Super plasticizer
- Galvanized steel welded wire mesh: 13 x 13 mm opening and 1mm diameter
- PVA fiber

3.3 Testing of Materials

After having procured the materials, different tests have to be conducted as follows:

- Cement - Consistency, initial and final setting time, and Specific gravity of cement as per IS 1489 (Part I) 1991(Reaffirmed 2005)
- Fine aggregates - Specific gravity, Water absorption, fineness modulus, sieve analysis and bulk density as per IS 383-2016 and IS 2386 (Part III) – 1963(Reaffirmed 2002)
- Wire mesh - The Uni-axial tension test on reinforcement bars is performed as per IS 1608-2005

3.4 Mix Design of Self Compacting Normal Mortar

The research incorporates self-compacting (SC) mortar materials, which consist of ordinary Portland cement, fly ash, and fine aggregate. To ensure the desired workability, superplasticizers are also included. The selection of these constituent materials has been carried out meticulously to achieve the necessary compressive strength for the mortar.

In this study, the mix design for SC mortar has been specifically tailored to target a strength of 45 MPa. The preparation and testing of the mortar will primarily focus on evaluating its mechanical properties, aiming to ensure its suitability for the intended application.

For clarity and reference, Table 3.1 presents the precise proportions of the constituent materials used in the mix design for the self-compacting mortar. These proportions have been carefully determined to achieve the desired performance characteristics and meet the specified compressive strength requirements.

3.5 Casting SC Normal Mortar Ferrocement I-Beam Specimens

The research includes the casting of monolithic I-beam specimens using ferrocement. These I-beam specimens are specifically designed to have dimensions as depicted in Figure 3.1. The intention behind casting these specimens is to evaluate and analyze the structural behavior and performance of ferrocement in the form of I-beams.

Figure 3.1 provides a visual representation of the prescribed dimensions of the I-beam specimens. These dimensions have been carefully determined to ensure the accurate

representation of an I-beam structure, considering factors such as span length, flange width, flange thickness, and web height.

By casting and testing these monolithic I-beam specimens, the research aims to gain insights into the mechanical properties, load-carrying capacity, and overall structural performance of ferrocement in the form of I-beams, contributing to a better understanding of its potential applications in construction and engineering.

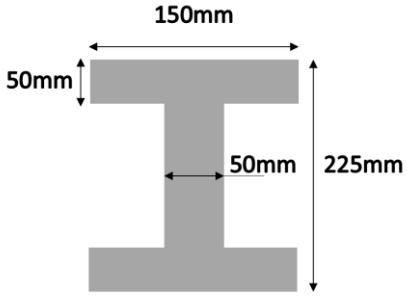

Figure 3.2 I-beam specimen

The flanges of the specimen will have a width of 150mm and a depth of 50mm, while the web will have a length of 125mm and a depth of 50mm. To reinforce the specimen, a welded wire mesh will be positioned through the center of the mortar matrix. This arrangement results in an effective depth of the I-beam of 200mm, while the total depth, including the wire mesh, is 225mm. The entire length of the specimen is 2000mm, providing a sufficient span for testing and analysis.

To facilitate the casting process, a proposed design for the mould is presented in Figure 3.2. The mould is constructed using iron members, ensuring durability and stability during the casting process. The detachable iron log is supported at both ends to maintain the desired shape of the I-beam.

Each component of the mould is designed to be easily assembled and disassembled using screws. This feature allows for convenient demoulding after the casting process is completed. Overall, this mould design provides a practical and efficient solution for casting the I-beam specimen monolithically, enabling accurate evaluation of the ferrocement's structural performance and behavior.

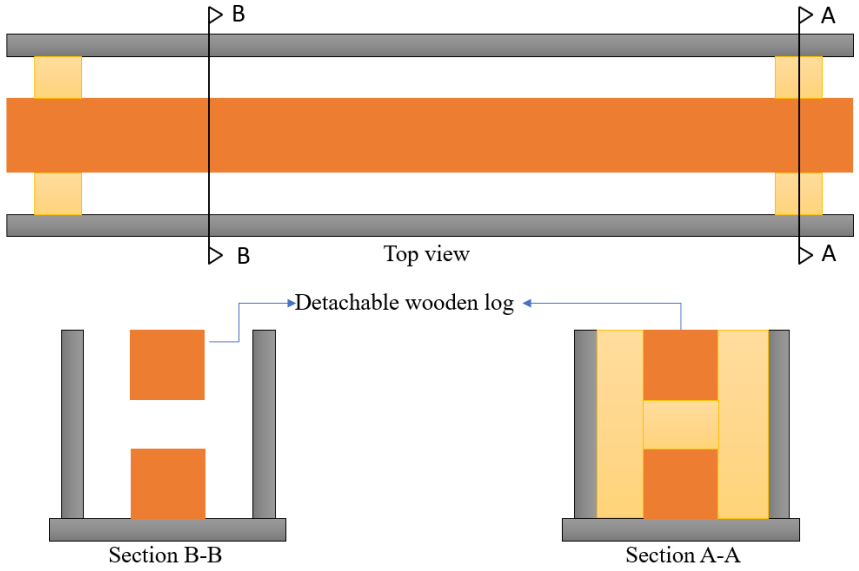

Figure 3.3 Design of mould

3.6 Flexural Testing of SC Normal Mortar Ferrocement I-Beam

The I-beam specimens of ferrocement will be subjected to a two-point loading test within a 200 KN loading frame. This testing setup allows for the study of the behavior and performance of the ferrocement I-beams under applied loads. The test setup is illustrated in Figure 3.3.

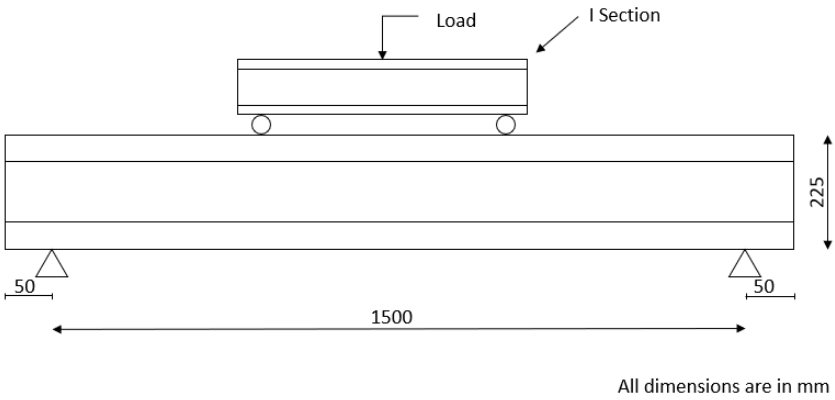

Figure 3.4 Test setup

During the two-point loading test, the beams will be supported at two points, and the load will be applied at the mid-span of the beam. The deflection of the beam at the mid-span will be measured using LVDTs (Linear Variable Differential Transformers). These measurements will be used to plot the load-deflection curve, providing valuable insights into the beam's structural response and deformation characteristics under load. Figure 3.4 shows the loading configuration used for this testing method. This arrangement ensures

a controlled and consistent application of load during the testing process, allowing for accurate data collection and analysis.

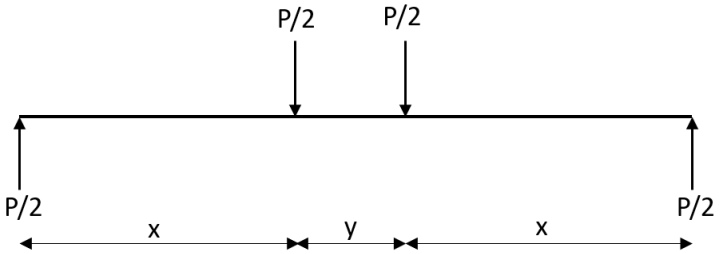

Figure 3.5 Loading configuration

By conducting these tests and obtaining load-deflection curves and moment-curvature relationships, the research aims to comprehensively assess the structural performance and behavior of the ferrocement I-beams, providing valuable information for engineering and construction applications.

3.7 Mix Design of Self Compacting ECC Mortar

The research will utilize Engineered Cementitious Composites (ECC) as the material of interest. The constituents selected for the ECC mixture include ordinary Portland cement, fly ash, fine aggregate, and an optimal amount of fibers. Superplasticizers will also be incorporated into the mixture to enhance workability and flowability. The proportions of these constituent materials will be carefully chosen to achieve the desired compressive strength of the ECC. It is crucial to attain the specified strength requirement to ensure the structural integrity and performance of the material.

In the ECC mix, coarse aggregates are intentionally excluded as their presence can have a detrimental effect on the ductility of the mixture. Coarse aggregates tend to increase crack width, which is contradictory to the desired property of ECC. The absence of coarse aggregates helps to maintain the desirable characteristics of ECC, such as high tensile strain capacity and enhanced crack control. The mix design for ECC will be formulated to achieve a target strength of M40, indicating a compressive strength of 40 MPa. This particular strength level is selected to meet the requirements of the intended application and ensure the ECC's ability to withstand the expected loads and stresses.

By carefully selecting and proportioning the constituent materials, as well as excluding coarse aggregates, the ECC mixture will be tailored to exhibit excellent ductility, crack

resistance, and strength, making it a promising material for various structural applications.

3.8 Casting SC ECC I-Beam Specimens

The research includes casting monolithic I-beam specimens using Self-Compacting Engineered Cementitious Composites (SC ECC) with ferrocement reinforcement. The dimensions of these SC ECC I-beam specimens will be the same as those of the control specimen. To ensure consistency and comparability, the same mould used for casting the control specimen will also be employed for casting the SC ECC I-beam specimens.

By utilizing the same mould, any variations or discrepancies due to differences in moulding techniques or mould design will be minimized, allowing for a more accurate comparison between the control specimen and the SC ECC I-beam specimens. This approach ensures that any observed differences in structural behavior and performance can be primarily attributed to the incorporation of SC ECC and ferrocement reinforcement, rather than experimental variables associated with the moulding process.

Through this casting method, the research aims to evaluate and analyze the structural characteristics, mechanical properties, and performance of the SC ECC I-beam specimens, providing insights into the potential application of SC ECC with ferrocement reinforcement in structural engineering and construction.

3.9 Flexural Testing of SC ECC Ferrocement I-Beam

The SC ECC ferrocement I-beam specimens will undergo a two-point loading test within a 200 KN loading frame. This testing method enables the study of the structural behavior and performance of the SC ECC ferrocement I-beams under specific loading conditions. To ensure a comprehensive analysis, all the calculations performed for the control specimen will be repeated for the SC ECC ferrocement I-beam specimens. This includes evaluating the structural properties, such as the moment of inertia, section modulus, and other relevant parameters. By performing these calculations, the research aims to determine the expected structural response and performance of the SC ECC ferrocement I-beams.

During the two-point loading test, the beams will be supported at two points, and the load will be applied at the mid-span of each specimen. This loading configuration allows for a controlled and standardized application of load, facilitating accurate data collection and

analysis. The behavior of the SC ECC ferrocement I-beams will be closely observed and monitored during the test. Various measurements, such as deflection, strain, and load, will be recorded to assess the structural response and performance of the beams under the applied load. By repeating the calculations and conducting thorough testing on the SC ECC ferrocement I-beam specimens, the research aims to gain a deeper understanding of their behavior, mechanical properties, and structural performance. This information can contribute to the development and application of SC ECC ferrocement in practical engineering projects.

3.10 Result Analysis

Indeed, the results obtained from the testing of all the specimens, including the control specimen and the SC ECC ferrocement I-beam specimens, will be carefully analysed. The analysis will comprehensively examine the collected data, considering various factors such as load-deflection behavior, strain distribution, and overall structural performance. By comparing and contrasting the results from different specimens, meaningful insights can be gained regarding the behavior and performance of the SC ECC ferrocement I-beams compared to the control specimen. The data analysis will involve statistical analysis, graphical representation, and interpretation of the results.

The aim of the analysis is to identify any notable differences, advantages, or limitations exhibited by the SC ECC ferrocement I-beams in comparison to the control specimen. Factors such as load-carrying capacity, deflection behavior, cracking patterns, energy absorption, and other relevant properties will be evaluated to draw meaningful conclusions. Based on the comprehensive analysis of the results, a suitable conclusion will be drawn regarding the suitability and effectiveness of SC ECC ferrocement I-beams in practical applications. This conclusion will be supported by empirical evidence and scientific observations obtained from the testing and analysis phase of the research.

The ultimate goal is to contribute to the existing knowledge base and provide valuable insights for the utilization of SC ECC ferrocement in structural engineering and construction practices.

Chapter 4

Experimental Investigation

4.1 General

The main focus of the present project was to assess the feasibility and effectiveness of utilizing Ferrocement I beams as structural members. Additionally, the project aimed to investigate the potential improvement in beam performance by replacing the matrix with Engineering Cementitious Composite (ECC).

4.2 Materials Used for Experiments

4.2.1 Cement

The research project utilized Ordinary Portland Cement (OPC) of 53 grade from the CHETTINAD cement brand, which adheres to the IS:12269:1987 standard. OPC Grade 53 is commonly preferred in construction and plastering applications due to its exceptional strength and durability. OPC Grade 53 cement is well-suited for projects that require high compressive strength, making it a popular choice for structural elements that need to withstand heavy loads. Its composition and manufacturing process result in a cement with finer particles and a lower proportion of impurities, contributing to its superior performance.

One significant advantage of OPC Grade 53 cement is its faster initial setting time compared to Portland Pozzolana Cement (PPC). The initial setting time refers to the duration taken for the cement to begin hardening after water is added. The shorter setting time of OPC Grade 53 cement allows for quicker work progress in construction activities, enabling efficient project timelines. To ensure the quality and conformity of the cement used, material tests were conducted on the OPC Grade 53 cement. These tests validate its compliance with the specified standards and confirm its suitability for the intended applications.

Figure 4.1 Cement

By utilizing OPC Grade 53 cement in the research project, the aim is to leverage its high strength, durability, and faster setting time, thereby enhancing the overall quality and reliability of the experimental findings and conclusions.

4.2.2 Fine Aggregate

In the research project, M Sand is utilized as the fine aggregate in the design mix. M Sand, or manufactured sand, is a substitute for natural river sand and is widely used in construction projects. It is produced by crushing hard granite or basalt rocks into fine particles. The primary purpose of incorporating M Sand in the design mix is to fill the voids between the coarse aggregate particles, enhancing the overall density and compactness of the concrete or mortar mixture. This helps in achieving sufficient strength and durability of the resulting structure.

Various tests are conducted to evaluate the characteristics of the M Sand. Some of these tests include Specific Gravity Test which determines the density of M Sand in comparison to the density of water. It provides valuable information about the quality and uniformity of the sand particles. Gradation Test which refers to the distribution of particle sizes. This test helps in determining the proportion of different particle sizes present in the sand, which can impact the workability and strength of the mixture. Fineness Modulus Test which is calculated based on the gradation test results. It provides an indication of the average particle size of the sand and helps in evaluating its suitability for the desired concrete or mortar mix.

Figure 4.2 Fine aggregate

By conducting these tests on M Sand, the research project aims to assess its specific gravity, gradation, fineness modulus, and other relevant characteristics. This information enables proper selection and utilization of M Sand in the design mix, ensuring the desired strength, durability, and workability of the resulting structure.

4.2.3 Fly Ash

In the ECC mix, Type F fly ash is employed due to its pozzolanic nature and high silica content. Fly ash is a byproduct of coal combustion in power plants and is commonly used as a supplementary cementitious material in concrete mixes. Type F fly ash is particularly beneficial in ECC mixes because of its pozzolanic properties. When mixed with calcium hydroxide, which is present in the cement paste, fly ash reacts to form additional cementitious compounds. This reaction leads to increased strength and durability of the ECC.

One of the advantages of using fly ash in ECC is that it can help reduce the cement content while maintaining or even improving the ductile properties of the mixture. By replacing a portion of the cement with fly ash, the overall cementitious material content in the ECC mix can be increased. This higher cementitious content contributes to improved workability, flowability, and bond strength in the absence of coarse aggregates. Furthermore, the incorporation of fly ash in the ECC mix can enhance the material's resistance to alkali-silica reactions. The high silica content in fly ash reacts with alkalis present in the mix, reducing the potential for harmful chemical reactions that can lead to cracking and deterioration.

Figure 4.3 Fly ash

By utilizing Type F fly ash in the ECC mix, the research aims to optimize the cementitious material content, enhance the ductility of the mixture, and improve overall performance. This approach not only reduces the reliance on cement but also contributes to sustainable construction practices by utilizing a supplementary material like fly ash.

4.2.4 PVA Fibre

In the research project, Polyvinyl Alcohol (PVA) fibers are utilized as high-performance reinforcement fibers for concrete and mortar. PVA fibers are known for their excellent crack-fighting properties and are commonly used to enhance the durability and performance of the material. The PVA fibers used in the project have a length of 12mm and a diameter of 39μm. These fibers are added to the concrete or mortar mix to improve its structural properties and provide reinforcement at a microscopic level.

PVA fibers possess several desirable characteristics that make them suitable for this application. Some of these characteristics include Superior Crack-Fighting Properties which is the ability to distribute stresses and prevent the formation and propagation of cracks within the concrete or mortar. This helps enhance the overall durability and lifespan of the structure.

High Modulus of Elasticity which allows them to resist deformation under applied loads, maintaining the structural integrity of the material. Excellent Tensile and Molecular Bond Strength enabling them to withstand significant forces and contribute to the overall strength of the composite material and to have a strong molecular bond with the cement matrix, ensuring effective reinforcement.

PVA fibers are resistant to alkali attack, which can occur in the presence of alkaline substances in the concrete or mortar mix. This resistance ensures the long-term stability

and performance of the reinforced material. PVA fibers help control and minimize the formation and width of cracks, enhancing the material's resistance to cracking due to shrinkage, temperature changes, or other external factors.

Figure 4.4 PVA fiber

By incorporating PVA fibers with the specified length and diameter, the research project aims to harness their crack-fighting properties, high modulus of elasticity, excellent tensile and molecular bond strength, alkali resistance, and cracking resistance. This utilization of PVA fibers contributes to improved performance, durability, and structural integrity of the concrete or mortar.

4.2.5 Limestone Powder

In the self-compacting mortar used in the research project, limestone powder with a specific gravity of 2.7 is incorporated. Limestone powder serves to enhance the flowability and workability of the mortar due to its fine particle size. The fineness of the limestone powder allows it to fill in the voids between the particles of other constituents, such as cement and aggregates. This results in improved particle packing and increased lubrication within the mortar mixture. As a result, the mortar becomes more fluid and exhibits enhanced flowability.

By adding limestone powder to the self-compacting mortar, the research project takes advantage of its flow-enhancing properties. The improved flowability not only facilitates ease of placement and compaction but also contributes to achieving a uniform distribution of the mixture within the formwork. Additionally, limestone powder is commonly used as a filler material in mortars and concrete due to its availability and cost-effectiveness. Its incorporation helps optimize the overall composition and performance of the self-compacting mortar while utilizing a readily available and sustainable material.

Figure 4.5 Limestone powder

Overall, the inclusion of limestone powder in the self-compacting mortar improves its flowability and workability, enabling efficient and effective placement and compaction processes during construction activities.

4.2.6 HRWR

Cera hyperplast XR-W40 is a polycarboxylate ether-based High Range Water Reducer (HRWR) utilized in the research project. It possesses a specific gravity of 1.06 and a pH of 6. The dosage of this HRWR typically falls within the range of 0.7 to 1.8, depending on the specific requirements of the mixture.

The primary purpose of using Cera hyperplast XR-W40 as an HRWR is to enhance the performance and properties of the self-compacting mortar. Some notable benefits and effects achieved through its incorporation include High Early Strength, Workability Retention, Shrinkage and Creep Reduction, Low Water-Cement Ratio

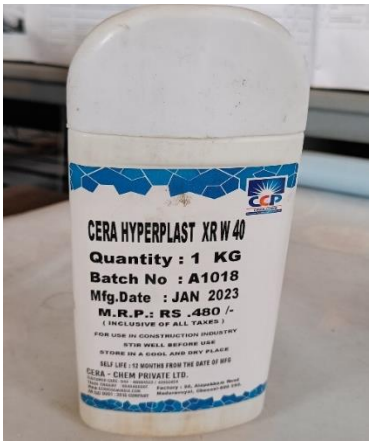

Figure 4.6 HRWR

By utilizing Cera hyperplast XR-W40 in the self-compacting mortar, the research project aims to harness its benefits, including high early strength development, workability retention, shrinkage, and creep reduction, as well as achieving a low water-cement ratio. These properties contribute to the overall performance and durability of the self-compacting mortar mixture.

4.2.7 Welded Wire Mesh

For the research project, a welded wire mesh is employed, made of galvanized steel with a size of 19 gauge. The mesh features square openings measuring 13mm x 13mm. Galvanized steel is chosen as the material for the wire mesh due to its corrosion resistance and durability. The galvanization process provides protection against rust and extends the lifespan of the wire mesh. The wire mesh possesses specific mechanical properties, including a yield stress of 287.5 MPa and an ultimate stress of 357.69 MPa.

Figure 4.7 Welded wire mesh

By utilizing a welded wire mesh with these mechanical properties, the research project aims to enhance the structural integrity, reinforce the self-compacting mortar or concrete, and improve crack control. The wire mesh acts as a reinforcement element, increasing the overall tensile strength and improving the resistance to cracking and deformation within the material.

4.2.8 Water

In the research project, potable water was used, which means water suitable for drinking. The water used in the project was ensured to be free from oils, acids, and any organic

matter. The research project adhered to the guidelines specified in IS 456:2000, which is the Code of Practice for Plain and Reinforced Concrete.

According to IS 456:2000, the pH value of the water should be less than 6. pH is a measure of the acidity or alkalinity of a solution. By specifying a pH value below 6, the code ensures that the water used in construction does not have excessive alkalinity, which can adversely affect the properties of the concrete or mortar. Adhering to these guidelines and using potable water free from oils, acids, and organic matter, the research project aimed to maintain the quality and consistency of the concrete or mortar mixture. This helps in achieving the desired strength, durability, and overall performance of the construction material.

4.3 Experimental Works on Materials

4.3.1 Tests on Cement

Fineness test on cement

The fineness test of cement serves as an important measure of particle size distribution, providing valuable insights into the quality and consistency of the cement used in construction. In this research project, the fineness test was conducted following the guidelines outlined in IS 4031-Part 1. The test involved sieving a 100g sample of cement through a standard 90-micron sieve. The initial weight of the cement sample was denoted as W1. The sieving process was carried out for a duration of 15 minutes, ensuring a thorough and representative evaluation of the cement particles. After sieving, the weight of cement retained on the 90-micron sieve was measured and recorded as W2. This measurement provides information on the proportion of cement particles that exceed the specified sieve size, indicating the relative fineness of the cement.

Fineness of cement = (W_2/W_1) x 100

The fineness test results for the cement sample obtained in this research project indicate a value of 1.5%. According to the IS specification, the maximum allowed value for the fineness of cement is 10%. Therefore, the obtained value of 1.5% complies with the requirements set by the IS specification.

Figure 4.8 Fineness test

By performing the fineness test, the research project aimed to assess the particle size distribution of the cement sample, which plays a crucial role in determining the workability, setting time, and overall performance of the resulting concrete or mortar mixture. The obtained results will contribute to ensuring the quality and suitability of the cement for construction purposes.

Standard consistency test on cement

The determination of the standard consistency of cement was carried out using the Vicat apparatus, in accordance with IS 4031-Part 4. The test involved the use of a plunger with dimensions of 50mm in length and 10mm in diameter. A 400g sample of cement was employed for the test. The gauging time for the cement paste was maintained between 3 to 5 minutes, ensuring a consistent testing environment. Various percentages of water were added to the cement, starting from 30%. The cement paste was then filled into a mould and placed under the plunger of the Vicat apparatus.

Upon releasing the plunger quickly, the penetration reading was noted. The water percentage required to achieve a penetration depth of 5 to 7mm from the bottom was recorded. In this particular test, the standard consistency obtained was 32%. Comparing this result with the recommended value specified in the IS Specification, which suggests a range of 26% to 33% for achieving a penetration depth of 5 to 7mm, it can be concluded that the obtained standard consistency conforms to the IS Specification.

Figure 4.9 Standard consistency test

By conducting the standard consistency test, the research project ensures that the appropriate water content is determined for the cement paste, facilitating optimal workability, setting time, and overall performance of the resulting concrete or mortar mixture.

Initial setting time test

When water is added to cement, a chemical reaction called hydration takes place. This reaction causes the cement-water mixture to transition from a fluid state to a solid state, which is known as the setting of cement. In this research project, the initial setting time of cement was measured in accordance with IS: 4031 (Part 5) 1988, using the Vicat Apparatus with a needle measuring 1mm square in size. For the test, 400g of cement and 0.85 times the amount of water required for standard consistency were used to create the cement paste.

The gauging time for the cement paste was maintained between 3 to 5 minutes to ensure consistent test conditions. After filling the mould with the paste, the Vicat needle was placed on top and quickly released, allowing it to penetrate the cement. The time elapsed between adding water to the cement and the point at which the 1mm square section needle failed to penetrate the cement to a depth of about 5mm from the bottom of the mould was recorded as the initial setting time. In this specific test, the initial setting time obtained was measured as 45 minutes. Comparing this result with the requirement specified in the IS Specification, which states that the initial setting time should be greater than 30 minutes, it can be concluded that the obtained initial setting time conforms to the specified requirement.

Figure 4.10 Initial setting time

By measuring the initial setting time, the research project ensures that the cement has the desired setting characteristics, providing insights into the appropriate workability, setting time, and overall performance of the resulting concrete or mortar mixture.

Specific gravity test on cement

To determine the specific gravity of cement, the following apparatus are used: LeChatelier flask, kerosene or naphtha free from water, and a weighing balance. The procedure is conducted as follows:

- Ensure that the LeChatelier flask is thoroughly dried and clean. Fill the flask with kerosene oil or naphtha up to a point on the stem between zero and one millilitre. The inside of the flask above the liquid level should be dried.
- Immerse the flask in a water bath maintained at a constant room temperature and allow it to equilibrate for a sufficient period.
- Record the initial reading of the level of kerosene in the flask.
- Introduce approximately 64 grams of cement into the flask in a manner that causes the level of kerosene to rise above the base portion. Care should be taken to prevent the cement from adhering to the sides of the flask above the liquid.
- Insert the stopper into the flask and gently roll it in an inclined position. This action expels any air from the cement until no air bubbles rise to the surface of the liquid.
- Note the final reading of the level of kerosene in the flask.

The observations taken include the weight of the cement used, as well as the initial and final readings on the flask. The volume of cement is calculated by subtracting the initial reading from the final reading.The specific gravity of the cement is determined using the following formula:

Specific Gravity = Weight of Cement / Displaced volume of kerosene in ml

The specific gravity of the cement sample obtained in this research project is measured as 3.12. Comparing this value with the permissible range specified in the IS specification, which is 3.12 to 3.19, it can be concluded that the obtained specific gravity value conforms to the IS specification.

Figure 4.11 Specific gravity of cement

By following this procedure, the specific gravity of the cement can be accurately determined. This information is valuable for assessing the quality and properties of the cement, aiding in the appropriate design and formulation of concrete or mortar mixtures.

4.3.2 Tests on Fine Aggregate

Specific gravity test on fine aggregate

The specific gravity of fine aggregate was determined using a pycnometer bottle. The following weights were measured and noted during the test:

W1 = Weight of pycnometer = 626 g

W2 = Weight of pycnometer + sand = 1125 g

W3 = Weight of pycnometer + sand + water = 1840 g

W4 = Weight of pycnometer + water = 1526 g

Specific gravity, $G = \frac{W_2 - W_1}{(W_2 - W_1) - (W_3 - W_4)} = 2.7$

Obtained value of specific gravity for fine aggregate = 2.7

The specific gravity of the fine aggregate obtained in this research project falls within the range specified by IS 2386-Part 3, which is 2.65 to 2.85. This indicates that the specific gravity value of the fine aggregate conforms to the IS specification.

Figure 4.12 Specific gravity of sand

By conforming to the IS specification, the research project ensures that the fine aggregate meets the required quality standards. This, in turn, contributes to the overall quality, workability, and durability of the construction material.

Particle size distribution of fine aggregate

The particle size distribution of the fine aggregate was determined using the mechanical method known as sieve analysis, as prescribed in IS 2386-Part 1. The following procedure was followed to obtain the coefficients of uniformity and curvature and to draw the grain size distribution curve:

- Sieve Selection: Sieves of various sizes, including 4.75mm, 2.36mm, 1.18mm, 600µ, 300µ, and 150µ, were selected for the sieve analysis.
- Sample Preparation: A representative 1 kg sample of M-Sand (fine aggregate) was taken for analysis.
- Sieving Process: The fine aggregate sample was sequentially sieved through the selected sieves. After each sieving, the weight of the material retained on each sieve was measured and recorded. The weight retained was expressed as a

percentage of the total sample weight, indicating the percentage finer than the respective sieve size.

- Graph Plotting: A graph was plotted using the percentage finer (Y-axis) and the sieve size (X-axis). This graph represents the grain size distribution curve of the fine aggregate.
- Effective Size and Coefficients Calculation: From the semi-logarithmic graph, the effective size of the particles was determined. The uniformity coefficient and coefficient of curvature were calculated using the obtained particle size distribution data.

Figure 4.13 Sieve Analysis of Fine Aggregate

Table 4.1 Particle Size Distribution Table of Fine Aggregate

Sieve Size	**Weight Retained in Each Sieve**	**Percentage Weight Retained**	**Cumulative % Weight Retained**	**% Weight Passing**
4.75mm	2	0.2	0.2	99.6
2.36mm	142	14.2	14.4	85.6
1.18mm	242	24.2	38.6	61.4
600µ	210	21	59.6	40.4
300µ	248	24.8	84.4	15.6
150µ	118	11.8	96.2	3.8
Pan	38	3.8	100	0

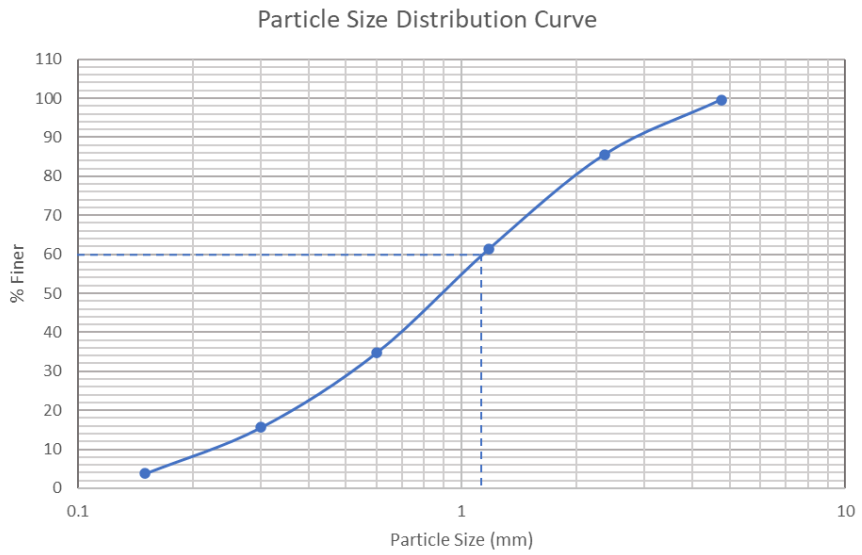

Figure 4.14 Particle Size Distribution Curve of Fine Aggregate

From the Figure 5.1,

D_{10} = 0.23

D_{30} = 0.52

D_{60} = 1.15

Uniformity Coefficient, $C_u = \frac{D_{60}}{D_{10}} = \frac{1.15}{0.23} = 5$

Coefficient of curvature, $C_c = \frac{{D_{30}}^2}{D_{60} \times D_{10}} = \frac{0.52^2}{1.15 \times 0.23} = 1.02$

Based on the graph and the calculated values, it can be determined that the fine aggregate belongs to Zone 2. This classification is based on the values of the coefficient of uniformity (Cu) falling between 4 and 6 and the coefficient of curvature (Cc) falling between 1 and 3.

4.3.3 Tests on Fly Ash

Specific gravity of fly ash was measured by using pycnometer bottle. Following weights were measured and noted:

W1 = Weight of pycnometer = 665 g

W2 = Weight of pycnometer + fly ash = 715 g

W3 = Weight of pycnometer + fly ash + water = 1595g

W4 = Weight of pycnometer + water = 1567 g

Specific gravity, $G = \frac{W_2 - W_1}{(W_2 - W_1) - (W_3 - W_4)} = 2.27$

Obtained value of specific gravity for fly ash = 2.27

According to IS 3812.1.2003, the specific gravity of fly ash falls within the range of 2.1 to 3. By comparing this range with the specific gravity value obtained in the research project, it can be concluded that the specific gravity of the fly ash conforms to the IS specification.

4.4 Mix Preparation

Self-Compacting Engineered Cementitious Composite (SC ECC) is a specialized type of cementitious material that is designed for self-compaction and enhanced performance. The composition of SC ECC typically includes cement, fly ash, silica, sand, water, a small amount of admixtures, and an optimal amount of fibers. In the formulation of SC ECC, the exclusion of coarse aggregates is intentional. Unlike traditional concrete mixes, SC ECC is designed to exhibit the formation of multiple microcracks. These microcracks contribute to the unique properties of SC ECC, such as improved ductility, enhanced crack resistance, and reduced permeability.

Self-Compacting Normal Mortar is a specialized type of mortar designed for self-compaction and ease of application. It is composed of cement, sand, limestone powder, water, and a small amount of admixtures. The cement provides binding properties and strength, while the sand serves as the fine aggregate. Limestone powder enhances flowability and workability. Water activates the cement's hydration process. Admixtures improve specific properties.

4.5 Mix Compositions

Table 4.2 Mix composition of SC Normal Mortar mix (Abdulla 2022)

Cement	Limestone filler	Sand	Water
596.4	89.46	1192.8	208.74

Table 4.3 Mix composition of SC ECC (Dinh 2022)

Cement	Fly Ash	Sand	PVA	Water
595.18	687.81	467	21.42	320

4.6 Tests Conducted

4.6.1 Slump Flow Test and T_{50} Test

The slump flow is used to assess the horizontal free flow of SCC. The test method is based on the test method for determining the slump. The diameter of the concrete circle is a measure for the filling ability of the concrete.

Figure 4.15 Slump flow and T_{50} test

For this test, a mould in the shape of a truncated cone with the internal dimensions 200 of a stiff non absorbing material, at least 700mm square, marked with a circle marking the central location for the slump cone, and a further concentric circle of 500mm diameter, trowel, scoop, ruler, stopwatch (optional) are required. About 6 litre of concrete, normally sampled is needed to perform the test. The base plate and inside of slump cone is moistened and the slump cone is placed centrally on the base plate kept on level stable ground and hold down firmly. The cone is filled with the scoop. Surplus concrete is removed around the base of the cone if any. The cone is raised vertically and the concrete is allowed to flow out freely. Simultaneously, the stopwatch is srarted and recorded the time taken for the concrete to reach the 500mm spread circle (Tso time). The final diameter of the concrete is measured in two perpendicular directions. The average of the two measured diameters gives the slump flow in mm.

The higher the slump flow (SF) value, the greater its ability to fill formwork under its own weight. A value of at least 650mm is required for SCC. The T_{50} time is a secondary indication of flow. A lower time indicates greater flowability. It is suggested that a time of 3-7 seconds is acceptable for civil engineering applications, and 2-5 seconds for housing applications.

4.6.2 Compressive Strength (Cube Specimen)

Compression tests were conducted on specimens of Self Compacting ECC and Self Compacting Normal Mortar in accordance with the specifications outlined in IS: 516-1959. The specimens used for testing had dimensions of 70.6 mm x 70.6 mm x 70.6 mm. The average strength of three trial cubes was recorded at both 7 and 28 days. The compression tests were performed using a compression testing machine with a capacity of 2000N. The machine, as illustrated in Figure 4.16, was utilized to apply compressive loads to the specimens and measure their corresponding strength values. Three samples of each mix, namely Self Compacting ECC and Self Compacting Normal Mortar, were tested to determine their average compressive strength.

Figure 4.16 Compressive strength test

4.6.3 Split Tensile Strength

The splitting tensile strength test is a widely recognized method for determining the tensile strength of concrete. In this research project, the test was conducted on cylindrical concrete specimens with a diameter of 150 mm and a height of 300 mm, following the specifications outlined in IS: 5816-1999. To perform the splitting tensile strength test, a compression testing machine with a capacity of 3000 kN was employed as shown in

figure 6. The concrete cylinder was positioned with its axis perpendicular to the loading surfaces and the load was applied gradually until the failure occurred, resulting in a splitting failure along the plane that contains the vertical diameter of the specimen. This test was carried out at the 28th day of casting The values are recorded and split tensile value (T_{sp}) obtained by:

$$T_{sp} = \frac{2P}{\pi dl}$$

Where,

P = maximum loads in Newtons applied to the specimen

l = supported length (cm)

d = Diameter of specimen (cm)

Figure 4.17 Split Tensile Strength Test

4.6.4 Modulus of Elasticity

To evaluate the modulus of elasticity, the procedures outlined in IS 516-1959 were followed. The 28th day SC ECC cylinder specimen and SC Mortar specimen were subjected to compression testing using a compression testing machine with a capacity of 3000 kN, as shown in Figure 4.18.

The compression load applied to the specimens was set at 75% of the compressive strength of cube specimens. A compressometer, with a gauge length of 200 mm, was attached to the specimens to measure the longitudinal deformations corresponding to the applied loads.

By dividing the dial gauge reading by the gauge length, the strain values were obtained. The load applied was divided by the cross-sectional area of the specimen to calculate the corresponding stresses. Using the collected data, a stress-strain curve was plotted. The slope of the curve represents the modulus of elasticity, which is a measure of the material's stiffness and ability to deform under applied loads.

Figure 4.18 Compression Test on ECC Specimen for Modulus of Elasticity

4.6.5 Density

The research project involved conducting tests on 28-day strength cube specimens of both the mixes, namely SC ECC and SC Normal Mortar. These cube specimens were specifically selected for evaluating the density of the materials. The density of a material is determined by calculating the ratio of its mass to its volume. In this case, the mass of the cube specimens was measured using a weighing balance, while the volume was determined by measuring the dimensions of the cubes. By dividing the mass of the cube specimen by its corresponding volume, the density of the material can be obtained. The density value provides valuable information about the compactness and mass per unit volume of the material.

4.7 Casting of Ferrocement I Beam

Ferrocement I Beam specimens of SC ECC and SC Normal Mortar are made of particular dimensions as shown in figure 3.2

4.7.1 Mixing

In the case of SC ECC mix to ensure the optimal performance of the composite and achieve a homogeneous fiber dispersion, a systematic sequence was followed during the mixing process. The dry materials, including cement, fly ash, and fine aggregate, were initially dry-mixed for a duration of 2 minutes in a Pan-type concrete mixer with double rotation. This dry-mixing process allowed for the uniform distribution of the dry components. Next, water and the High Range Water Reducing (HRWR) admixture were added to the dry materials, and the mixing process continued for an additional 3 minutes. This step ensured that the water and admixture were thoroughly incorporated into the mixture. Finally, the Polyvinyl Alcohol (PVA) fibers were introduced into the mix. Care was taken to add the fibers gradually while mixing to prevent clumping and to ensure proper dispersion throughout the mixture. The mixing process was extended for another 5 minutes to ensure that the fibers were uniformly dispersed and no clusters were visible. After the mixing process, the prepared mixture was cast into lightly oiled moulds. The application of a light oil coating facilitated easy demoulding of the samples after they had cured.

Figure 4.19 Pan type concrete mixer

Figure 4.20 Dry mixing

To ensure proper mixing and homogeneity in the SC Normal Mortar mix, a systematic process was followed. Initially, the dry materials, which included cement, limestone powder, and fine aggregate, were dry-mixed for a duration of 1.5 to 3 minutes in a pan type concrete mixer. This dry mixing allowed for the uniform distribution of the dry components, ensuring consistency in the mixture. After the dry mixing, water and the High Range Water Reducing (HRWR) admixture were added to the dry materials. The

mixing process was continued for an additional 3 minutes to thoroughly incorporate the water and admixture into the mixture. This step ensured that the water-to-cement ratio and the HRWR admixture were properly dispersed throughout the mix, promoting workability and desired properties. Once the mixing process was complete, the prepared mortar mixture was cast into lightly oiled moulds. The application of a light oil coating on the moulds facilitated easy demoulding of the samples after they had cured. This step aided in the smooth and efficient removal of the specimens from the moulds without causing any damage or distortion.

4.7.2 Casting of Test Specimen

During the concrete mixing process, a pan type mixer was utilized to ensure proper homogeneity and uniform distribution of the ingredients. The mixer facilitated the thorough blending of cement, aggregates, water, and any other admixtures required for the specific mix design. To prepare the moulds for casting, the bottom and inner sides were coated with oil. This oil coating prevented the concrete from sticking to the moulds, facilitating easy demoulding after curing. Careful attention was given to the placement of the reinforcement mesh, ensuring it was properly positioned within the mould. Adequate covering, both at the bottom and sides of the reinforcement mesh, was maintained to ensure proper bond and reinforcement integrity within the concrete. The mixed concrete matrix was then carefully placed into the melds, taking care to avoid any segregation or air entrapment. The top surface of the specimens was given special attention, ensuring a level and finished appearance. This step involved smoothing and levelling the concrete surface to achieve a consistent and visually appealing finish.

Figure 4.21 Reinforcement arrangement

Figure 4.22 Placing of reinforcement mesh in the mould

After 72 hours of casting, the specimens were demoulded from the moulds. Special care was taken to handle the freshly demoulded specimens to prevent any damage or distortion. Following demoulding, the specimens were subjected to a moist curing process for a duration of 28 days. Jute bags were used to cover the specimens during curing, promoting a moist environment conducive to proper hydration and strength development. To facilitate the observation of crack patterns during testing, the cured specimens were white washed. This surface treatment enhanced the visibility of cracks and provided valuable insights into the structural behavior of the specimens under load. The testing of the beams was conducted on the 28th day of casting, following the completion of the curing process. This time frame allowed for sufficient strength development and ensured that the specimens were ready for testing and evaluation.

Figure 4.23 Casted specimen

Figure 4.24 Demoulded specimen

Figure 4.25 Curing

4.8 Experimental Setup

The beam specimens were subjected to a testing setup where they were simply supported at two ends, with one end serving as a fixed roller support and the other as a free roller support. Steel rollers with a diameter of 40 mm were utilized for both roller supports. Prior to testing, the positions of the supports, load points, and midpoint were marked on the beam. The beam was carefully placed over the supports in the loading frame,

following the marked positions. It was ensured that there was a clearance of 50 mm beyond the support and a clear distance of 1500 mm between the supports. The level of the beam was checked using a level tube to ensure proper alignment. Loading of the beam was achieved by employing a hydraulic jack with a capacity of 200 kN. The jack was securely fixed to the loading frame using a C-clamp. The position of the beam was adjusted to ensure the plumb line through the center of the jack coincided precisely with the center line of the beam. To maintain the loading rate, a load cell was positioned between the jack and the beam.

For the study, a two-point loading configuration was adopted, with the load being applied at a distance of 25 mm from the middle of the beam. To transfer the load to the beam without inducing bending in the transfer beam, an I-beam with a length of 1.50 m was utilized. The center of the spreader beam was aligned with the plumb line through the jack. Safety precautions were taken by loosely tying the spreader beam and load cell to the frame using ropes to avoid any accidents. To measure the deflection at each load increment, three dial gauges with 0.01 mm accuracy were placed at both load points and the midpoint of the bottom portion of the beam. The plunger portion of the dial gauges was set to touch the bottom surface of the glass sheet, and the initial dial reading was set to zero. A magnifying glass was used to identify cracks on the beam, while a micrometre microscope with a 0.1 mm accuracy was employed to measure the crack width. The laboratory setup for the test is depicted in Figure 4.26, illustrating the arrangement of the beam, supports, jack, spreader beam, load cell, dial gauges, and measurement instruments.

Figure 4.26 Test setup

4.9 Testing of Beam Specimens

After the beams had undergone a curing period of 28 days, the testing phase commenced. The load was applied manually by pumping the hydraulic jack. Initially, a seating load was given to the beam, and the readings of the dial gauges were taken corresponding to the zero load condition. The load was then incrementally increased, and the readings of the dial gauges were recorded at each load increment.The load at which the first crack appeared on the beam was carefully noted. The cracks that developed on the beam were marked according to their chronological order. The propagation of cracks during the loading process was closely observed and documented. As the cracks on the beam widened, the dial gauges were removed from their respective positions. The loading was continued until the beam eventually failed, and the load at failure was noted. Additionally, the widths of the cracks were measured and recorded. Throughout the testing process, the behavior of the beam under load, including crack development and failure, was thoroughly observed and documented. This data is crucial for analyzing the performance and structural integrity of the beams.

Chapter 5

Results and Discussion

5.1 General

The tests were conducted in accordance with the procedures described in the previous chapter and the results and discussions are presented in this chapter.

5.2 Test Results

The compressive strength, modulus of elasticity, splitting tensile strength and density of the SC ECC mix and SC Normal Mortar mix were carried out and the results were compared.

5.2.1 Slump Flow Test and T_{50} Test

The slump flow value and the T_{50} time for both mixes are given in Table 5.1

Table 5.1 Slump flow value and T_{50} time

Mix	**Slump flow value (mm)**	**T_{50} time (sec)**
SC Normal Mortar	675	5
SC ECC	725	4

According to IS 10262, a self-compacting mix should exhibit a slump flow of at least 650 mm and a T50 time (the time taken for the concrete to reach 500mm spread circle) between 3 and 7 seconds. Both the SC ECC and SC Normal mortar mixes satisfied these conditions, indicating their ability to achieve the desired flowability and workability. This compliance with the specified slump flow and T50 time requirements demonstrates the effectiveness of the mixes in terms of self-compacting properties, allowing for easier and more efficient placement and consolidation during construction.

5.2.2 Compressive strength

The average cube compressive strength for both mixes is given in Table 5.2

Table 5.2 Average cube compressive strength for both mixes

Mix	**Compressive Strength (N/mm^2)**	
	7 day	**28 day**
SC Normal Mortar	20.4	44.52
SC ECC	18.7	44.65

Comparing the results of compressive strength of both the mixes it was found that both the mixes shows almost the same compressive strength as both the mixes were prepared to attain the same compressive strength of 45Mpa in 28 days.

5.2.3 Split tensile strength

For splitting tensile strength, cylinders were cast and tested for 28 days. Table 5.3 shows the comparison of splitting tensile strength for both mixes.

Table 5.3 Split tensile strength of mixes

Mix	**Split Tensile Strength (N/mm^2) after 28 days of water curing**
SC Normal Mortar	4.7
SC ECC	10.9

The tensile strength of the SC Normal mortar mix was determined to be 10.6% of its compressive strength. On the other hand, the split tensile strength of the SC ECC mix was found to be 24.4% of its compressive strength. This significant improvement in tensile strength observed in the SC ECC mix can be attributed to the incorporation of PVA fibers into the mix. The presence of PVA fibers enhances the tensile properties of the ECC, resulting in a higher split tensile strength compared to the SC Normal mortar mix. This improvement in tensile strength is advantageous for the structural performance of the SC ECC, making it a promising material for various applications.

5.2.4 Modulus of Elasticity

The modulus of elasticity for both mixes was obtained from the load-deflection diagram obtained during the test conducted. Table 5.4 presents the values of the modulus of elasticity for each mix.

Table 5.4 Modulus of elasticity of mixes

Mix	Modulus of elasticity (GPa) after 28 days of water curing
SC Normal Mortar	25.31
SC ECC	28.58

The modulus of elasticity of the SC ECC mix was found to be slightly higher than that of the SC Normal Mortar mix, which can be attributed to the presence of PVA fibers in the SC ECC mix. The inclusion of PVA fibers enhances the overall stiffness and strength of the mix, resulting in a higher modulus of elasticity. However, it is important to note that both the SC ECC mix and SC Normal Mortar mix exhibit lower modulus of elasticity compared to conventional concrete. This is primarily due to the absence of coarse aggregate in these mixes. Coarse aggregate provides rigidity and contributes to the higher modulus of elasticity typically observed in concrete.

5.2.5 Density

The average cube density for both mixes is given in Table 5.5

Table 5.5 Density of mixes

Mix	Density (g/cc)
SC Normal Mortar	2.14
SC ECC	1.98

The density of the SC ECC mix was found to be lower than that of the SC Normal Mortar mix, and this can be attributed to the presence of lightweight PVA fibers in the SC ECC mix. PVA fibers are known for their low density, which can contribute to a reduction in the overall density of the mix.

5.3 Summary of Test Results

Based on the analysis of the test results, it can be concluded that the SC ECC mix exhibits superior tensile strength characteristics compared to the SC Normal Mortar mix. This indicates that the inclusion of PVA fibers in the SC ECC mix has enhanced its ability to withstand tensile forces and resist cracking. Furthermore, despite having a lower density than the SC Normal Mortar mix, the SC ECC mix demonstrates comparable compressive

strength. This suggests that the SC ECC mix is capable of achieving similar levels of load-bearing capacity and structural integrity as the SC Normal Mortar mix, while offering the added advantage of improved tensile strength. Overall, the combination of enhanced tensile strength and comparable compressive strength makes the SC ECC mix a favorable material choice, particularly in applications where crack resistance and structural durability are important factors.

5.4 Test Results for Beams

The cube specimens cast during the casting of the I beams showed an average compressive strength of 44.35 Mpa and 43.98 for SC ECC I beam and SC Normal Mortar I beam respectively which almost complies with the values shown during mix preparation. The flexural behavior of the I beams was investigated through static loading. The specimens were subjected to two-point loading, inducing pure bending in the central zone. Deflection measurements were taken at the center and loading points throughout the experiment. The loads at which the first crack appeared were recorded, and the failure load was determined. Several parameters were examined during the testing, including deflection, ultimate load carrying capacity, ductility index, energy absorption characteristics, crack pattern, and crack width. Observations from the experiment were used to plot load-deflection graphs, providing insights into the structural response. The load-deflection graphs allowed for the calculation of pre-cracking stiffness and post-cracking stiffness. These values provide an indication of the beam's initial resistance to bending and its behavior after the onset of cracking. By analyzing these stiffness values, the beam's ability to withstand loads and distribute stresses can be evaluated.

5.4.1 Load-deflection characteristics

The values of deflection obtained at the mid-span and loading points for the I beams made of SC ECC mix and SC Normal Mortar mix are presented in Table 5.6 and Table 5.7, respectively. These measurements provide valuable data on the structural behavior of the beams under flexural loading. Using the recorded deflection values, load-deflection graphs were plotted for both types of beams, illustrating their respective load-deflection characteristics. The Load-deflection plots for the beams under flexure are depicted in Figure 5.2 and Figure 5.3. These graphs visually represent the relationship between the applied load and the resulting deflection, providing insight into the beam's response to bending forces. Furthermore, Figure 5.4 and Figure 5.5 offers a comparison of the mid-

span deflections and load point deflections respectively of the beams under flexure. This comparative analysis allows for a direct assessment of the deflection performance between the SC ECC mix and SC Normal Mortar mix beams

Table 5.6 Deflection of SC Normal Mortar ferrocement I beam

Load (N)	**Deflection (mm)**		
	Load Point 1	**Mid Span**	**Load Point 2**
0.980665	0.05	0.05	0.04
1.96133	0.12	0.12	0.1
2.941995	0.14	0.15	0.12
3.92266	0.17	0.17	0.15
4.903325	0.2	0.22	0.19
5.88399	0.24	0.26	0.22
6.864655	0.28	0.29	0.26
7.84532	0.31	0.33	0.29
8.825985	0.33	0.35	0.31
9.80665	0.36	0.36	0.34
10.787315	0.39	0.39	0.37
11.76798	0.43	0.45	0.42
12.748645	0.45	0.48	0.44
13.72931	0.49	0.51	0.48
14.709975	0.54	0.57	0.53
15.69064	0.56	0.6	0.57
16.671305	0.58	0.64	0.58
17.65197	0.64	0.68	0.65
18.632635	0.66	0.71	0.68
19.6133	0.72	0.75	0.73
20.593965	0.76	0.81	0.78
21.57463	0.84	0.91	0.87
22.555295	0.88	0.94	0.9

Table 5.7 Deflection of SC ECC ferrocement I beam

Load (N)	**Deflection (mm)**		
	Load Point 1	**Mid Span**	**Load Point 2**
0.980665	0.06	0.07	0.055
1.96133	0.135	0.15	0.13
2.941995	0.19	0.2	0.19
3.92266	0.24	0.315	0.24
4.903325	0.285	0.355	0.29
5.88399	0.35	0.455	0.365
6.864655	0.4	0.505	0.42
7.84532	0.46	0.595	0.475
8.825985	0.525	0.67	0.52
9.80665	0.575	0.735	0.58
10.787315	0.615	0.785	0.63
11.76798	0.655	0.835	0.685
12.748645	0.7	0.865	0.725
13.72931	0.735	0.915	0.77
14.709975	0.77	0.955	0.805
15.69064	0.805	0.975	0.83
16.671305	0.83	1.01	0.86
17.65197	0.845	1.05	0.88
18.632635	0.875	1.085	0.905
19.6133	0.895	1.14	0.935
20.593965	0.915	1.195	0.97
21.57463	0.94	1.225	0.995
22.555295	0.96	1.245	1.02
23.53596	1	1.305	1.05
24.516625	1.035	1.34	1.115
25.49729	1.08	1.395	1.17
26.477955	1.16	1.475	1.215
27.45862	1.235	1.56	1.285
28.439285	1.4	1.76	1.475
29.41995	1.625	1.96	1.775

30.400615	1.815	2.16	2.015
31.38128	2.01	2.385	2.17

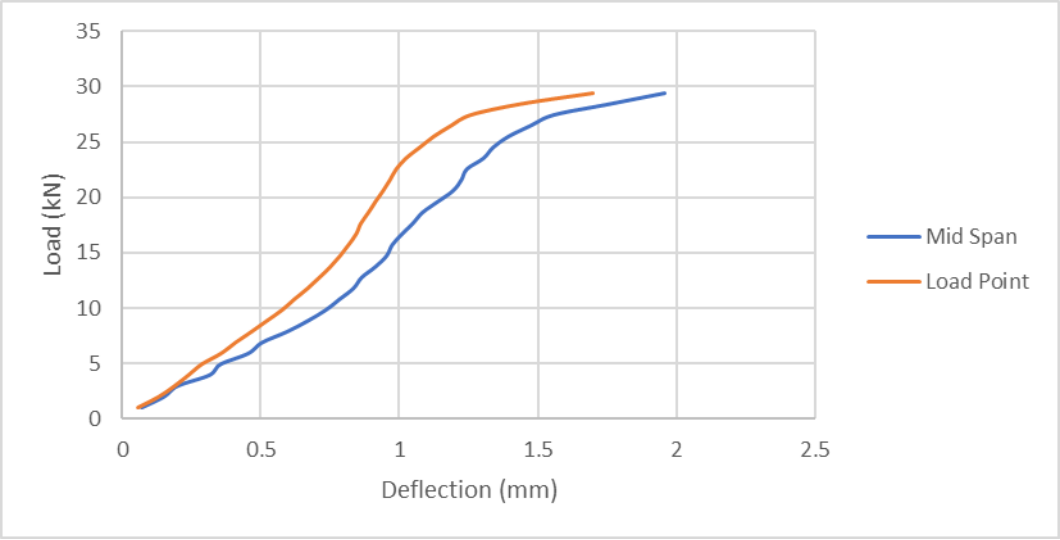

Figure 5.1 Load-deflection graph of SC ECC ferrocement I beam

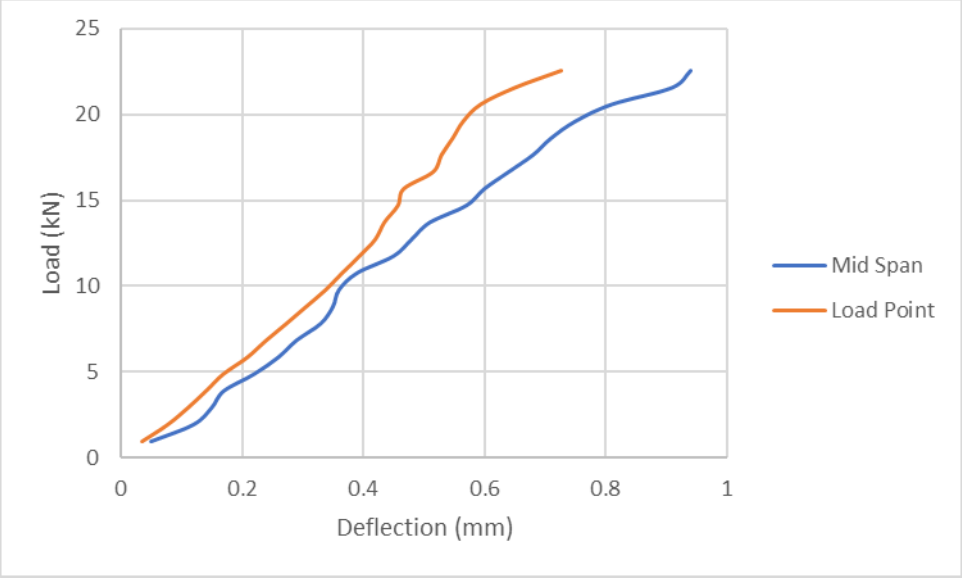

Figure 5.2 Load-deflection graph of SC Normal Mortar ferrocement I beam

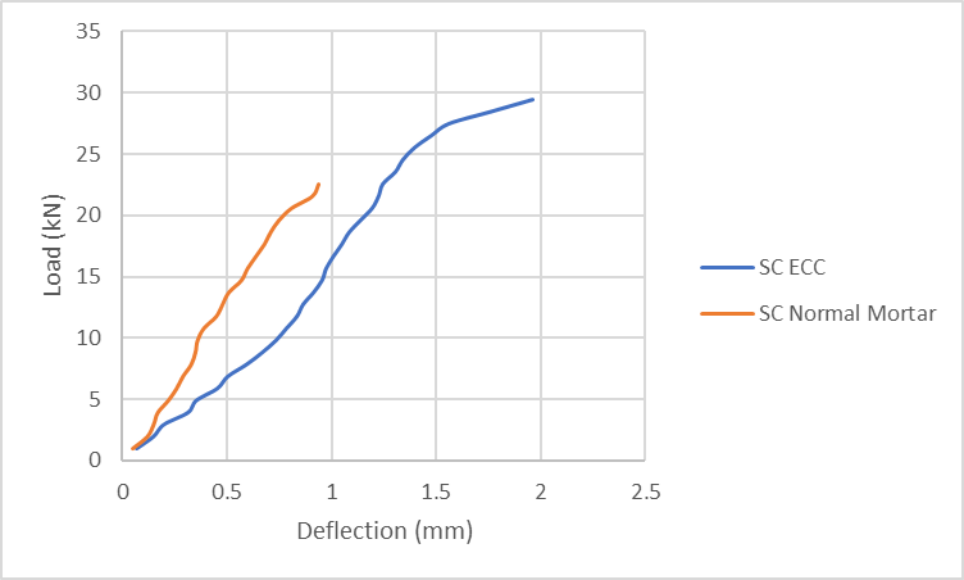

Figure 5.3 Load-deflection graph at mid span of beam specimens

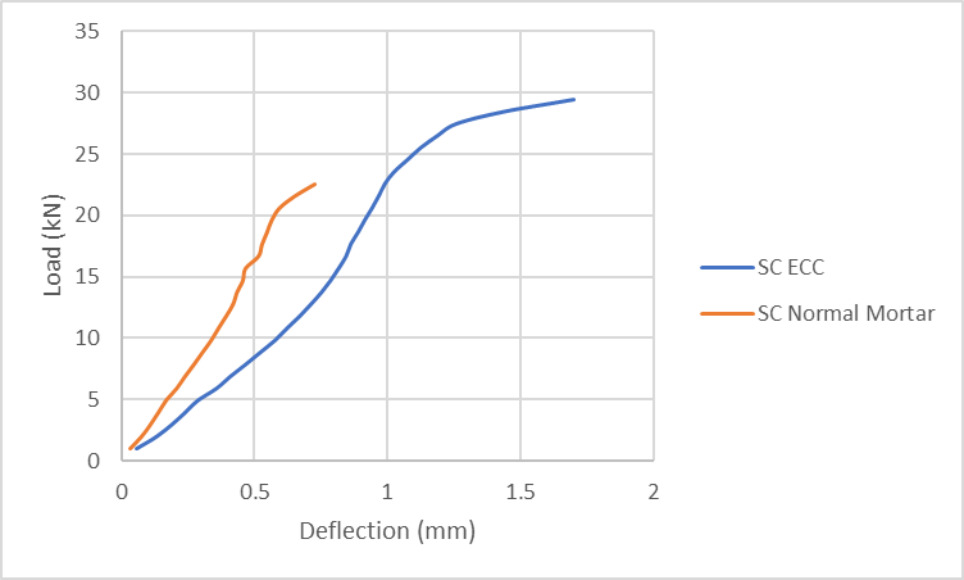

Figure 5.4 Load-deflection graph at load point of beam specimens

The experimental results clearly demonstrate that the SC ECC ferrocement I beam exhibits higher deflection at every point before failure compared to the SC Normal Mortar ferrocement I beam. This can be attributed to the bending nature of the Engineering Cementitious Composite (ECC) used in the SC ECC mix. ECC is known for its multiple cracking behavior and strain hardening effect, which allows for higher deflection capacity. On the other hand, although the SC Normal Mortar specimen demonstrates higher stiffness compared to the SC ECC specimen, it fails prematurely. This can be attributed to the limited ductility and crack width control of the SC Normal Mortar mix.

The absence of fibers in the SC Normal Mortar mix may contribute to its reduced capacity to withstand deformation and distribute stress.

The observed differences in deflection and failure behavior highlight the superior performance of the SC ECC ferrocement I beam compared to the SC Normal Mortar ferrocement I beam. The higher deflection capability of the SC ECC beam indicates its enhanced ability to absorb and dissipate energy, resulting in a more ductile and robust structural response.

5.4.2 Crack and Ultimate Load

The experimental results obtained from the flexure study provide valuable insights into the cracking behavior and load-carrying capacity of the SC ECC and SC Normal Mortar beam specimens. In the case of the SC ECC beam specimen, both the load at first crack and failure load were found to be greater compared to the SC Normal Mortar beam specimen. This can be attributed to the better mechanical properties of ECC, including its higher tensile strength and enhanced crack resistance. The ability of ECC to develop multiple microcracks helps to distribute stress more effectively, resulting in higher load-carrying capacity and improved performance.

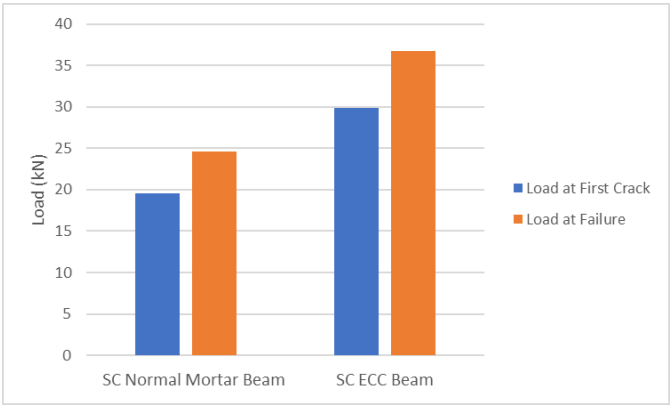

Figure 5.5 Variation of Cracking load and failure load

The variation of cracking load and ultimate load is depicted in Figure 5.5, illustrating the progressive failure behavior of the beams. Cracking initiation occurred at the middle third portion of the bottom flanges of the beams for both specimens. As the applied load increased, the cracks propagated rapidly from the bottom flanges through the web to the top flanges, and new cracks formed on either side of the beam centerline. The number of cracks observed in the SC ECC beam specimens was relatively lower compared to the SC

Normal Mortar beam specimen, which further highlights the superior tensile strength and crack resistance of ECC. The cracks formed in the SC ECC beam specimens were microcracks with widths below 0.1 mm, indicating the ability of ECC to effectively control crack width and limit crack propagation. In contrast, the average crack width observed in the SC Normal Mortar beam specimen was 0.2 mm, indicating a less controlled cracking behavior. Both the SC ECC and SC Normal Mortar beam specimens exhibited tension failure, and the cracking patterns were similar for both beams.

5.4.3 Margin between first cracking load and ultimate load

The margin between the first cracking load and ultimate load in flexure was calculated and compared for the SC ECC and SC Normal Mortar beams, and the results are presented in Table 5.8. It was observed that there was a delay in the initial crack formation within the SC ECC beams compared to the SC Normal Mortar beam. This indicates the improved crack resistance and enhanced load-carrying capacity of the SC ECC beams. Furthermore, the margin between the first cracking load and ultimate load was found to be higher for the SC ECC beams compared to the SC Normal Mortar beam. Specifically, the increase in the margin between the first cracking load and ultimate load for the SC ECC beams was 40% when compared with the SC Normal Mortar beam.

This significant increase in the margin indicates that the SC ECC beams have a higher capacity to sustain load even after the occurrence of the first crack. This can be attributed to the improved tensile strength and crack control properties of the ECC matrix in the SC ECC beams.

Table 5.8 Margin between first cracking load and ultimate load

Beam	**Load at first crack P_{cra} (kN)**	**Ultimate Load P_u (kN)**	**P_u /P_{cra}**	**Margin between P_u & P_{cra}**
SC Normal Mortar	19.61	24.51	1.24	4.9
SC ECC	29.91	36.77	1.22	6.86

5.4.4 Pre cracking and post cracking stiffness

The pre-cracking and post-cracking stiffness values for the beam specimens in the flexure study were calculated from the slope of the load-deflection curves. The pre-cracking stiffness was determined as the slope of the load-deflection curve up to the first cracking

point, while the post-cracking stiffness was calculated as the slope of the load-deflection curve after the occurrence of the first crack. The values of pre-cracking and post-cracking stiffness for the beam specimens are presented in Table 5.9. It was observed that the post-cracking stiffness was lower than the pre-cracking stiffness for all the beams, which is expected as the presence of cracks reduces the overall stiffness of the beam. This reduction in stiffness after cracking is a characteristic behavior of reinforced concrete structures.

In terms of a comparison between the SC Normal Mortar beam and the SC ECC beams, it was found that the SC Normal Mortar beam exhibited higher pre-cracking and post-cracking stiffness values compared to the SC ECC beams. This can be attributed to the composition and mechanical properties of the SC Normal Mortar mix, which may provide higher stiffness characteristics. Additionally, the ratio between the post-cracking and pre-cracking stiffness was higher for the SC Normal Mortar beam, indicating a greater ability to maintain stiffness after cracking. This may be due to the specific mix proportions and the presence of certain additives or admixtures in the SC Normal Mortar mix, which contribute to enhanced post-cracking stiffness.

Overall, the results suggest that the SC Normal Mortar beam exhibited higher stiffness values, both pre-cracking and post-cracking, compared to the SC ECC beams. However, it is important to note that the SC ECC beams demonstrated improved crack resistance and load-carrying capacity, as observed in the earlier analyses.

Table 5.9 Pre-cracking and post cracking stiffness

Beam	**Pre cracking stiffness, K_{pre} (kNmm)**	**Post cracking stiffness, K_{post} (kNmm)**	**K_{post}/K_{pre}**
SC Normal Mortar	24.6	9.8	0.39
SC ECC	24.5	4.92	0.20

5.4.5 Crack pattern and crack width

Cracking initiation in both the SC ECC and SC Normal Mortar beams occurred at the middle third portion of the bottom flanges. As the applied load increased, the cracks propagated from the bottom flanges through the web to the top flanges, and additional cracks formed on either side of the beam centerline. The cracking patterns observed in

both beams were similar, indicating a similar mode of crack propagation. However, there were notable differences in the visible number and width of cracks between the two specimens. The SC ECC beam specimens exhibited a lower number of visible cracks compared to the SC Normal Mortar beam specimen, indicating the superior tensile strength and crack resistance of ECC. The microcracks formed in the SC ECC beams had widths below 0.1 mm, which is significantly smaller than the average crack width of 0.2 mm observed in the SC Normal Mortar beam specimen. This suggests that ECC effectively controlled crack width and limited crack propagation, resulting in a more durable and resilient behavior. The ability of ECC to minimize crack formation and control crack width is attributed to its multiple cracking behavior and strain hardening effect. ECC is designed to develop microcracks, which distribute stress and reduce the risk of catastrophic failure. This behavior is particularly advantageous in improving the durability and longevity of structural elements. Crack pattern for the beams are shown in Figure 5.6 and Figure 5.7

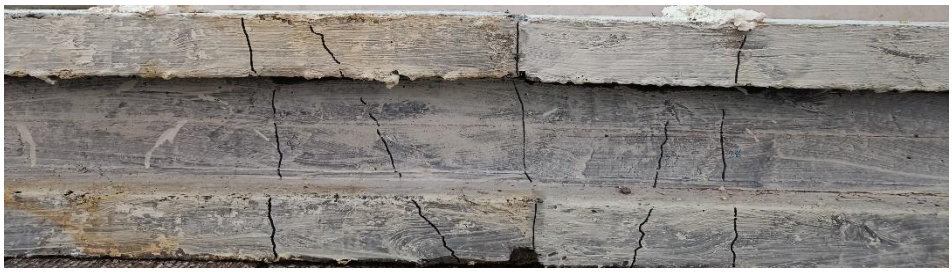

Figure 5.6 Crack pattern of SC ECC ferrocement I beam

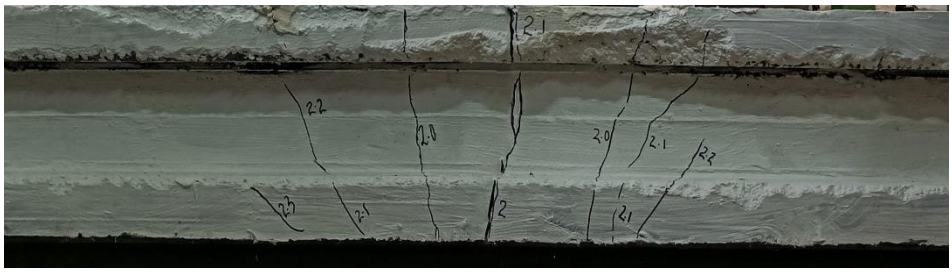

Figure 5.7 Crack pattern of SC Normal Mortar ferrocement I beam

Overall, the cracking behavior of the SC ECC beams demonstrated enhanced crack control and better crack resistance compared to the SC Normal Mortar beam specimen, highlighting the advantages of using ECC in structural applications.

5.4.6 Ductility index and energy absorption

Ductility plays a crucial role in the design of structures that are subjected to significant inelastic deformations caused by various loading conditions such as wind, seismic, or impact forces. It refers to the ability of a structural member to undergo deformations beyond the yield point without experiencing a significant reduction in its load carrying capacity. In the case of flexural members, the ductility can be determined from the load-deflection curve. It is quantified as the ratio of the deflection at the ultimate or failure point (Ymax) to the deflection at the first yielding of the tensile reinforcement (Yyield). This ratio provides a measure of the member's ability to sustain large deformations and redistribute stresses, thus improving its overall performance and resistance to failure. A higher ductility value indicates that the member can withstand substantial deformations before reaching its ultimate capacity, which is particularly important in structures exposed to severe loading conditions. By allowing for inelastic behavior and deformation capacity beyond the yield point, ductile members can effectively dissipate energy and provide a higher level of structural resilience and resistance to catastrophic failure.

In the experimental study, the ultimate deflection was defined as the deflection observed at the end of the test. To determine the yield deflection, the maximum load (Pmax) was first determined. A horizontal line parallel to the deflection axis was drawn through Pmax. Next, a secant line was drawn from the origin through a point corresponding to 0.75 Pmax on the load-deflection curve. The intersection of this secant line with the horizontal line passing through Pmax was considered as the yield point, and the corresponding deflection at this point was defined as the yield deflection. To assess the energy absorption capacity of the beam, the area under the load-deflection curve was calculated. This area represents the energy absorbed by the beam during the test and is commonly referred to as the energy to failure. Additionally, the energy dissipated at yield was determined by calculating the area under the load-deflection curve up to the yield deflection. The energy ratio was then calculated as the ratio between the energy to failure and the energy dissipated at yield. Figure 5.8 provides an illustrative representation of the above-described procedure for determining the yield deflection, energy absorption capacity, and energy ratio of the beam specimen.

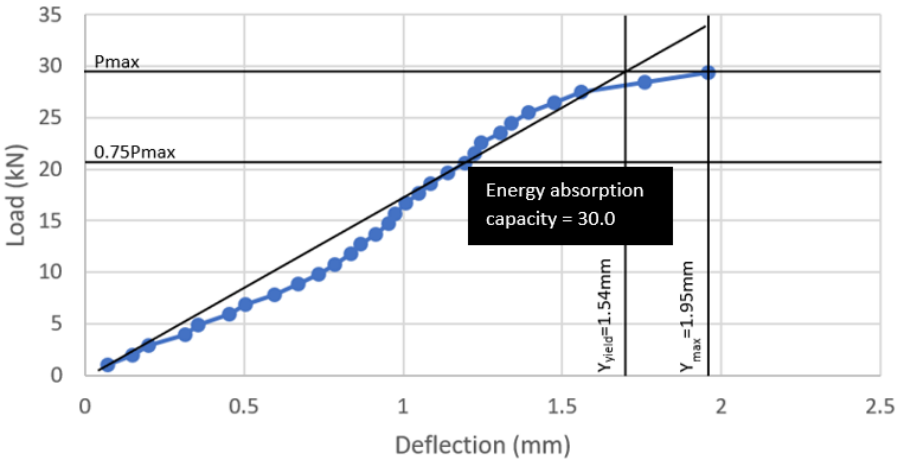

Figure 5.8 Load-deflection curve of SC ECC I beam during flexure test showing yield deflection and energy absorption capacity

Values of deflection at yield, ultimate deflection, ductility index and energy ratios for all the series of the beams tested are summarized in Table 5.10

Table 5.10 Energy absorption and ductility index

Beam	**Deflection at yield (mm)**	**Ultimate deflection (mm)**	**Ductility Index**	**Energy Absorption (Nm)**
SC Normal Mortar	0.85	0.94	1.11	10.60
SC ECC	1.54	1.95	1.27	30.00

The energy ratio for various beams for both tests is given in Table 5.11. Based on the results obtained, it can be concluded that the SC ECC I beam exhibits higher ductility and energy absorption capacity compared to the SC Normal Mortar I beam. The SC ECC I beam showed an increase in ductility of 14.41% and a significant increase in energy absorption of 183.01% compared to the SC Normal Mortar I beam in the flexure study. This indicates that the SC ECC I beam is able to undergo larger inelastic deformations without significant loss in its load carrying capacity, making it more resilient to loading conditions such as wind, seismic, or impact loads. The higher energy ratio observed for the SC ECC I beam further supports its superior energy absorption capability compared to the SC Normal Mortar beam.

Table 5.11 Energy ratio

Beam	**Energy to failure (Nm)**	**Energy to yield (Nm)**	**Energy ratio**
SC Normal Mortar	10.60	9.56	1.10
SC ECC	30.01	25.22	1.18

Chapter 6

Conclusion

The main objective of this investigation was to assess the ultimate load carrying capacity and flexural behavior of ferrocement I-beams using self-compacting normal mortar mix and ECC mix. The study aimed to determine the feasibility and effectiveness of utilizing ferrocement I-beams as structural members and to examine the differences in behavior when the SC Normal Mortar matrix is replaced with the SC ECC matrix. Additionally, the study investigated the load deformation characteristics and crack pattern development of the ferrocement I-beams.

Based on the results and observations, the following conclusions can be drawn:

- The SC ECC mix exhibited superior tensile strength characteristics compared to the SC Normal Mortar mix. The presence of PVA fibers in the ECC mix contributed to enhanced mechanical properties, including higher crack resistance and load carrying capacity
- The SC ECC beams demonstrated higher deflection under flexural loading compared to the SC Normal Mortar beams. This can be attributed to the bending nature of the ECC matrix, which allows for increased flexibility and deformation
- The increase in the margin between the first cracking load and ultimate load for the SC ECC beams was 40% when compared with the SC Normal Mortar beam, indicates that the SC ECC beams have a higher capacity to sustain load even after the occurrence of the first crack due to the improved tensile strength and crack control properties
- The SC Normal Mortar beams exhibited higher pre-cracking and post-cracking stiffness compared to the SC ECC beams. This indicates that the SC Normal Mortar beams had higher initial stiffness but were more prone to brittle failure, while the SC ECC beams exhibited greater flexibility and ductility
- The crack patterns observed in both types of beams showed cracking initiation at the middle third portion of the bottom flanges, with subsequent crack propagation through the web to the top flanges. The number of cracks was lower in the SC ECC beams, indicating improved crack resistance and tensile strength

- The SC ECC beams demonstrated better control over crack width, with microcracks below 0.1 mm, while the SC Normal Mortar beams exhibited wider cracks with an average width of 0.2 mm. This highlights the ability of ECC to effectively limit crack propagation and enhance durability
- The SC ECC I beam showed an increase in energy absorption of 183.01% compared to the SC Normal Mortar beam SC ECC I-beam. This suggests that the ECC mix is more capable of dissipating energy and can better withstand dynamic loading conditions
- The SC ECC I beam showed an increase in ductility of 14.41% compared to the SC Normal Mortar I beam. This implies that the ECC mix has a greater ability to undergo inelastic deformations without significant loss in its load carrying capacity

Based on these findings, it can be concluded that the use of ferrocement I-beams with SC ECC mix offers advantages in terms of higher tensile strength, improved crack resistance, and enhanced ductility compared to SC Normal Mortar mix. The results support the feasibility and effectiveness of utilizing ferrocement I-beams as structural members in construction projects.

References

[1] Abdullah, Qutaiba Najm, and Aziz I. Abdulla. "Flexural Behavior of Hollow Self Compacted Mortar Ferrocement Beam Reinforced by GFRP bars." *Case Studies in Construction Materials* (2022): e01556.

[2] Do, Tuong Dat Dinh, et al. "Impact of tension stiffening on the tensile and flexural behavior of ECC ferrocement." *Construction and Building Materials* 329 (2022): 127201.

[3] Dawood, Eethar Thanon, Abdalaziz Saad Shawkat, and Mafaz Hani Abdullah. "Flexural performance of ferrocement based on sustainable high-performance mortar." *Case Studies in Construction Materials* 15 (2021): e00566.

[4] Hung, Chung-Chan, Sherif El-Tawil, and Shih-Ho Chao. "A review of developments and challenges for UHPC in structural engineering: Behavior, analysis, and design." *Journal of Structural Engineering* 147.9 (2021): 03121001.

[5] Hung, Chung-Chan, Yueh-Ting Chen, and Cheng-Hao Yen. "Workability, fiber distribution, and mechanical properties of UHPC with hooked end steel macro-fibers." *Construction and Building Materials* 260 (2020): 119944.

[6] Hung, Chung-Chan, Chia-Wei Kuo, and Yi Shao. "Cast-in-place and prefabricated UHPC jackets for retrofitting shear-deficient RC columns with different axial load levels." *Journal of Building Engineering* 44 (2021): 103305.

[7] Sharma, Raju, and Prem Pal Bansal. "Experimental investigation of initially damaged beam column joint retrofitted with reinforced UHP-HFRC overlay." Construction and Building Materials 111 (2016) 408–418.

[8] Chung-Chan Hung, and Yu-Syuan Chen. "Innovative ECC jacketing for retrofitting shear-deficient RC members." *Journal of Building Engineering* 49 (2022): 103973.

[9] Shao, Yi, Chia-Wei Kuo, and Chung-Chan Hung. "Seismic performance of full-scale UHPC-jacket-strengthened RC columns under high axial loads." *Engineering Structures* 243 (2021): 112657.

[10] Deng, Mingke, Yangxi Zhang, and Qiqi Li. "Shear strengthening of RC short columns with ECC jacket: Cyclic behavior tests." *Engineering Structures* 160 (2018): 535-545.

[11] A.B.M.A. Kaish, M.R. Alam, and M. Jamil. "Improved ferrocement jacketing for restrengthening of square RC short column." Construction and Building Materials 36 (2012) 228–237.

[12] Xu, Ling-Yu, et al. "Enhancing long-term tensile performance of Engineered Cementitious Composites (ECC) using sustainable artificial geopolymer aggregates." *Cement and Concrete Composites* 133 (2022): 104676.
[13] Michael D. Lepech, and Victor C. Li"Water permeability of engineered cementitious composites." Cement & Concrete Composites 31 (2009) 744–753.
[14] Hu, Zhiheng, et al. "Local use of ECC to simultaneously enhance the shear strength and deformability of RC beams." *Construction and Building Materials* 353 (2022): 129085.
[15] Abdulkadir, Isyaka, et al. "Modelling and multi-objective optimization of the fresh and mechanical properties of self-compacting high volume fly ash ECC (HVFA-ECC) using response surface methodology (RSM)." *Case Studies in Construction Materials* 14 (2021): e00525.